# Picosecond Diffraction at the ESRF: How Far Have We Come and Where Are We Going?

Michael Wulff[@], Qingyu Kong[@], Marco Cammarata[@], Manuela Lo Russo[@], Philip Anfinrud[#], Friedrich Schotte[#], Maciej Lorenc[%], Hyotcherl Ihee[*], Tae Kyu Kim[*], Anton Plech[&]

[@]*European Synchrotron Radiation Facility, 6, rue Jules Horowitz, BP220, Grenoble 38043, France*
[#]*Laboratory for Chemical Physics, NIDDK, Building 5, National Institute of Health, Bethesda, MD 20892-0520*
[*]*Korea Advanced Institute of Science and Technology, 373-1 Gu-seong-dong, Yu-sung-gu, Daejeon 305-701, Republic of Korea*
[%]*Groupe Matière Condensée et Matériaux, Bat 11A, UMR CNRS 6626, Université de Rennes I, 35042 RENNES Cedex France*
[&]*Fachbereich Physik der Universitaet KonstanzUniversitaetsstrasse 10, 78457 Konstanz, Germany*

**Abstract.** The realization of solution phase pump-probe diffraction experiments on beamline ID09B is described. The pink beam from a low-K in-vacuum undulator is used to study the structural dynamics of small molecules in solution to 100 picosecond time resolution and at atomic resolution. The X-ray chopper and the associated timing modes of the synchrotron are described. The dissociation of molecular iodine in liquid $CCl_4$ is studied by single pulse diffraction. The data probe not only the iodine structures but also the solvent structure as the latter is thermally excited by the flow of energy from recombining iodine atoms. The low-q part of the diffraction spectra is a sensitive probe of the hydrodynamics of the solvent as a function of time.

**Keywords:** picosecond diffraction, single bunch exposures, pump-& probe diffraction, structural dynamics, in-vacuum undulators, choppers, toroidal mirror.
**PACS:** 31.70, 61.10, 82.53, 82.53

## INTRODUCTION

Real time observation of temporally varying molecular structures during chemical reactions is a great challenge due to their ultrashort time scales. Ultrafast optical spectroscopy operating on the pico- and femtosecond time scale has provided a wealth of information about the time scales in chemical reactions such as bond breakage, bond formation and electron and proton transfer [1]. Unfortunately the long wavelength of optical light, 300-700 nm, precludes direct structural information at the atomic/molecular level. Another technique is electron diffraction that gives access to the time domain from nano- to picoseconds [2,3]. However the short penetration depth of electrons makes it difficult to apply this technique in condensed matter, which is very important in biological and industrial problems. The third technique is time resolved X-ray diffraction [4] and X-ray spectroscopy [5], which is increasingly important due the many new synchrotrons such as the European Synchrotron Radiation Facility (ESRF) in Grenoble, the Swiss Light Source (SLS) in Villigen, The Advanced Photon Source (APS) in Argonne and Spring8 in Japan. In these facilities, intense and pulsed beams of X-rays are produced by undulators that enhance the intensity 1000 times over conventional bending magnets. This enormous increase leads to much shorter exposure times. The exposure time in a pink beam diffraction experiment on a small unit-cell protein is now in the microsecond range, i.e. comparable to the orbit time for an electron in the storage ring. If now the electrons in the storage ring are concentrated in one bunch, and if the associated X-ray pulse is isolated by a chopper, the exposure time is reduced to the X-ray pulse length, 100 ps, which is about $10^4$ times shorter than the open time of the chopper! The high bunch currents in the 4-bunch and 16-bunch mode at the ESRF are excellent for single pulse experiments.

The fastest time resolution is realized with pump & probe technology with reversible samples or samples that can be exchanged quickly. A subset of molecules is typically excited by femto or picosecond laser pulses and delayed X-ray pulses probe the evolving structures at that delay. By varying the laser/X-ray delay, snapshots of the moving molecules can be stitched together to form a film. The molecular structures are averaged over the 100 ps (fwhm) X-ray pulse, which is the limiting resolution of a synchrotron.

The time resolution in accelerator based X-ray science was recently dramatically improved at the Sub-Picosecond Pulse Source (SPPS) at Stanford where 80 fs X-ray pulses, produced in a linac, were used to probe an ultrafast solid-liquid phase transition in GaAs [6]. This experiment is a precursor for experiments at future X-ray Free Electron Lasers (XFEL) in the USA, Europe and Japan that are expected to produce ultrashort, coherent and semi-monochromatic (0.1%) X-ray pulses with up to $1 \times 10^{12}$ photons per pulse.

The purpose of this paper is to give a short description of the ultrafast X-ray diffraction facilities at the ESRF and discuss the recombination dynamics of iodine in liquid $CCl_4$.

## THE PULSED X-RAY SOURCE

Ultrafast time resolved experiments at the ESRF are done on beamline ID09B which is dedicated to pump & probe diffraction experiments. The X-rays are produced by a 236-pole in-vacuum undulator with a 17 mm magnetic period. At the minimum undulator gap, the deflection parameter K is 0.83 and the fundamental energy $E_f$, is 15.0 keV. The energy of ESRF electrons is 6.03 GeV. The undulator parameters at the fundamental energy are shown in Table 1 and the U17 spectra at 6.0 and 10.4 mm gap are shown in Fig 1.

**TABLE 1.** Source parameters for beamline ID09 (rms values, low-beta site ).

| Device | Sy($\mu$m) | Sz($\mu$m) | Sy'($\mu$rad) | Sz'($\mu$rad) | poles | Bmax(T) | Ef(keV) | Pcone(Watt/200mA) |
|--------|--------|--------|---------|---------|-------|---------|---------|-------------------|
| U17 | 56.5 | 10.2 | 87.9 | 7.5 | 236 | 0.54 | 14.8 | 386 |
| U20 | 56.5 | 10.2 | 87.9 | 7.5 | 200 | 0.75 | 8.8 | 710 |

The U17 undulator has three important features for time resolved experiments. $E_f$ can be tuned between 15 to 20 keV where diffraction experiments have the best trade-off between detected intensity and radiation damage. Secondly, the spectrum of the fundamental is quasi monochromatic with a $\delta E/E$ of 3.0 %. This pink beam can often be used without monochromator. Finally the heatload on the toroidal mirror and the chopper is modest, especially in the 4-bunch (40 mA) and the 16-bunch mode (90mA). At closed gap the U17 is used for Laue experiments from proteins. The toroidal mirror can focus $1.0\times10^{10}$ photons per pulse into a 100 x 60 um$^2$ spot. When the gap is opened to 10.4 mm, $E_f$ shifts to 19 keV and the second harmonic is reduced to 2% of the fundamental. This open-gap configuration is excellent for measuring transient structures in liquids.
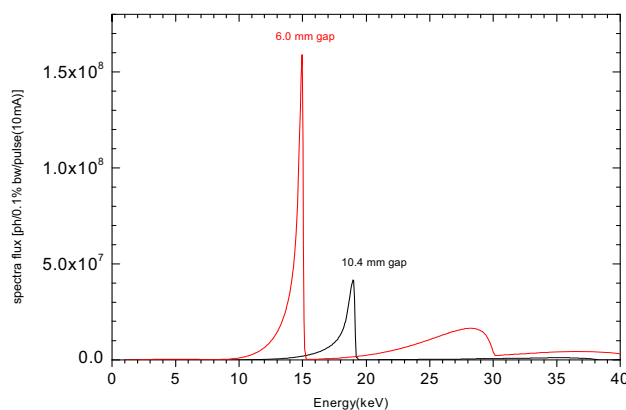


**FIGURE 1.** Spectral flux. from the U17 undulator. The flux is measured from a single bunch (10 mA) at 6.0 mm gap (Ef = 15 keV) and 10.4 mm gap (19.0 keV).

1188

The circumference of the ESRF storage ring is 844.1 m and it takes an electron 2.826 µs to traverse the ring at the speed of light. The orbit frequency is 355.042 kHz, but the radio frequency cavities (RF) at the ESRF operate at the 992 harmonic. In uniform filling of the ring, the electrons are evenly spaced and separated in time by 2.84 ns. This filling is not suitable for ultrafast experiments with CCD detectors since it impossible to select single pulses with a mechanical chopper from this densely filled pulse train. The solution is to use few-bunch fillings such as 4-bunch, 16-bunch or hybrid modes. In the four-bunch mode, which runs 4% of the time at ESRF, four 10 mA pulses are evenly spaced by 705 ns. A 10 mA bunch produces an intense flash with about $1 \times 10^{10}$ photons per pulse. The 4-bunch mode is excellent for Laue diffraction from proteins where the repeat frequency of the experiment is low due to laser heating. The lifetime is low, 6 hours, due to Coulomb repulsion within the bunch **(Touschek Effect)**. The pulse length is 150 ps (fwhm) at 10 mA and it reduces to 120 ps at the end of a fill at 6 mA. The 16-bunch mode runs 17% of the time at ESRF, and this structure is well suited for stroboscopic liquid experiments where the pulse sequence can be repeated at 1000 Hz by exchanging the sample between shots. At the injection, the current per bunch is 5.5 mA and the lifetime 12 hours. The bunch length starts at 110 ps and ends at 90 ps at 3.5 mA. The longer lifetime improves the stability of the focused beam, in space and in time. The pulse profile of a 16-bunch pulse is shown in Fig. 2.
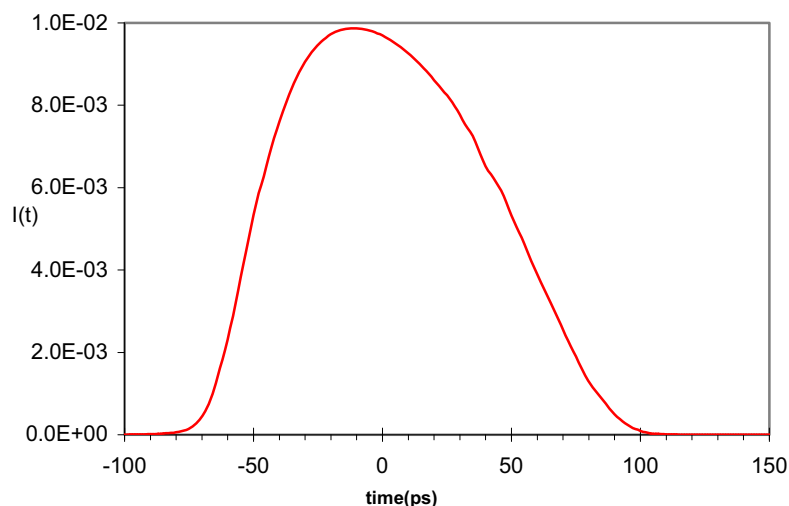


**FIGURE 2.** Temporal pulse profile in the 16-bunch mode. The current is 4.7 mA and the pulse is 104 ps wide (fwhm). Note that the rising edge is sharper that the falling edge. The measurement was made with the jitter-free streak camera on ID09.

# THE FOCUSING MIRROR

The central cone of the undulator is focused by a 1.0 m long cylindrical mirror, which is made from a single crystal of silicon. The mirror is placed 33.1 m from the source where the beam is 6.8 mm wide and 0.6 mm high (fwhm). The mirror is coated by platinum for improved reflectivity at high energy. The incidence angle is 2.668 mrad and energies between 0-26 keV are reflected. The sagittal radius is 71.6 mm. The beam is focused 22.4 m downstream into a spot size of 100 µm x 60 µm spot (fwhm). The mirror body is held at the ends and the shape is controlled by a spring-loaded stepper motor mounted below the mirror. The mirror dimensions are chosen such that gravity curves the mirror into a toroid that focuses the beam 22.4 m downstream ($R_m$=9.9 km). The measured longitudinal slope-error is as low as 0.7 µrad (rms). The mirror is water cooled through copper plates that are dipped into indium-gallium filled channels along the sides of the optical surface, see Fig. 3. The liquid interface between the mirror body and the cooling system attenuates vibrations from the cooling system. The $I_0$ stability measured through a 60 µm vertical slit at the focus is a good as $2 \times 10^{-3}$. The mirror parameters are discussed in depth in [7].
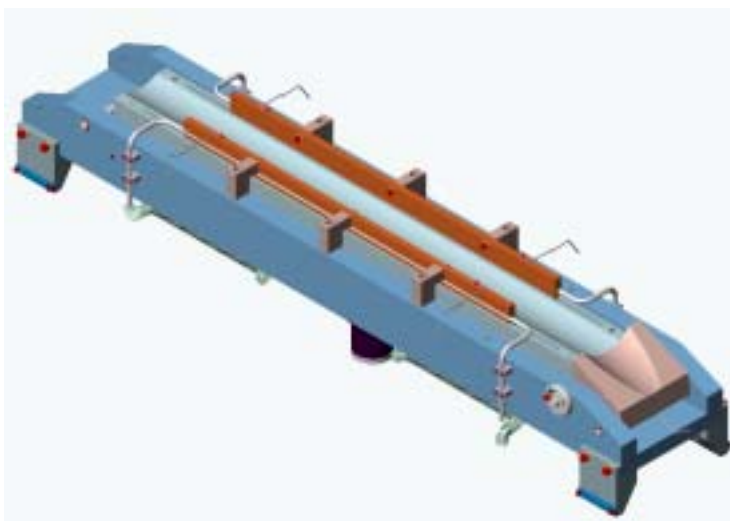
1189

**FIGURE 3.** The toroidal mirror and its cooling and bending system. The vertical curvature is adjusted by a spring-loaded stepper motor below the mirror.

## CHOPPER FOR SINGLE-PULSE SELECTION

One of the challenges in pump & probe experiments at synchrotrons is to control the pulse structure on the sample. The frequency of the X-ray pulses from the 16-bunch mode is 5.7 MHz, which is much faster than commercial femtosecond lasers that typically operate at 1 kHz. IN experiments with integrating CCD detectors, the laser/X-ray pulses have to arrive on the sample in pairs, i.e. the X-ray frequency has to be lowered to that of the laser. The solution is to use a chopper in front of the sample where the chopping efficiency is high due to the small beam size.

The ID09 chopper consists of a flat triangular disk that rotates in magnetic bearings in vacuum about the axis perpendicular to the disk, see Fig.4. It is designed by Bernd Lindenau and Jürgen Räbiger from KFA-Jülich in collaboration with ID09B staff. One of the three edges of the disk has a shallow channel that terminates with small roofs. The channel is thus a semi-open tunnel with slits at the ends. When the X-ray pulse is selected, the tunnel is parallel to the direction of the beam. The advantage of having a tunnel is that the beam envelope is cut from below and above simultaneously which reduces the open-time by two as compared with having the beam cut by the edges of a tunnel-less triangle.
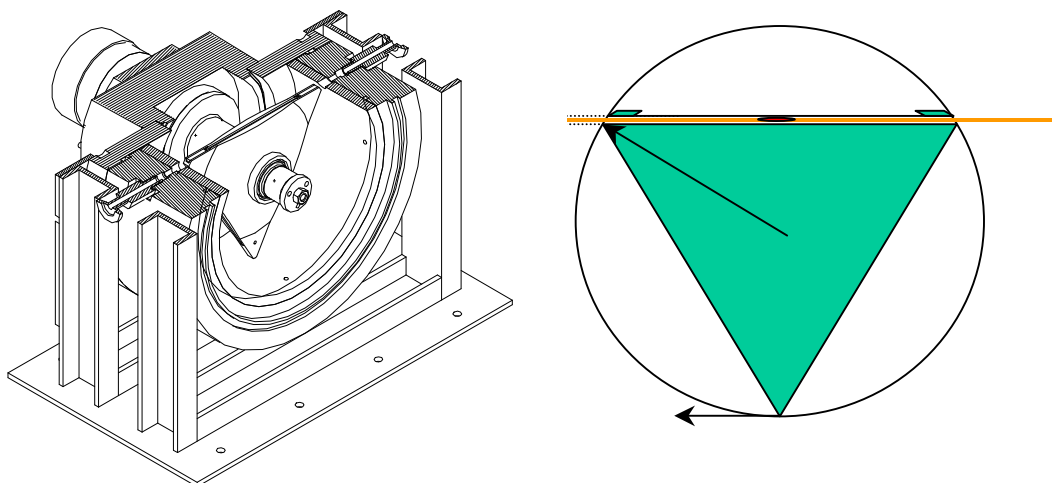


**FIGURE 4.** Chopper for single pulse selection. The semi-open tunnel geometry is shown on the right (vertical plane).

1190

If the radius of the triangle is r, the height of the tunnel h and the rotation frequency f, the (maximum) open time is

$$\Delta t = \frac{1}{\sqrt{3}} \frac{h}{\pi \, r \, f} \tag{1}$$

The chopper parameters are: r = 96.8 mm, h = 0.12 mm and f = 986.3 Hz giving $\Delta t$ = 225 ns. In 16-bunch mode where pulses are separated by 176 ns and the 225 ns open window is centered on the given pulse. The clearance to neighboring pulses is thus 63.5 ns. The measured jitter in the rotation is 3-4 ns (rms) which effectively suppresses the neighbor pulses. The open time can be changed slightly by moving the chopper horizontally: the tunnel has a trapezoidal cross section and the tunnel height varies from 0.05 mm to 0.9 mm over its 4.0 mm width. This geometry makes the open time variable from 96 to 1732 ns, which makes it possible to adapt to different bunch structures.

The chopper selects pulses continuously at 986.3 Hz, and produces hence a pulse every 1.014 ms. Protein crystals can't run this fast due to the heatload from the laser. In the case of myoglobin, hemoglobin and PYP, the highest frequency we have used is 3.3 Hz. For these "single-shot" experiments, the x-ray and the laser are gated by a millisecond shutter. The ms-shutter is installed in vacuum upstream the chopper. It consists of a 60 mm long bar with a tunnel along its length. The cross section of the tunnel is trapezoidal: it is 5 mm wide and the height increases linearly from 0.3 to 2.0 mm. The bar is rotated by a stepper motor. The shortest opening time is 0.2 ms, which is obtained by rotating the tunnel from –90 to +90 degree. The stepper motor requires 48 ms to move from –90 degree to the open position at 0 degree and this delay is stored in the software that controls to data collection.

## VISUALISING ATOMIC MOTIONS IN LIQUIDS

One of the first elementary reactions probed by X-rays was the recombination of dissociated iodine atoms in liquid $CCl_4$ [8-10]. A dilute $I_2/CCl_4$ (1: 360) solution was pumped by a femtosecond green laser pulse (150 fs, 520 nm) that promotes the iodine molecule from its ground state X to the excited states A, A', B and $^1\pi_u$. The emerging picture from numerous laser spectroscopy and X-ray diffraction studies is the following. The excited $I_2$ molecule dissociates rapidly into two neutral atoms that bounces violently in the solvent cage for a few picoseconds. These hot atoms recombine either geminately (a) or non-geminately (b):

$$I_2 + h\nu \rightarrow I_2^* \;\; , \; I_2^* \rightarrow I_2(a) \, , \, I_2 \rightarrow 2I \rightarrow I_2(b) \tag{2}$$
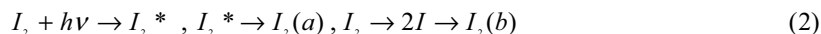
The geminate channel takes 86% of the excited $I_2^*$ molecules. Among them 77% recombine to the ground state in 180 ps and the remaining 23% are trapped in the A/A' state for 2.7 ns after which they decay to the ground state in 180 ps. The non-geminate fraction recombines diffusively in 22 ns. During the course of recombination, the solvent cools the solutes. This process is adiabatic for times up to 1 millisecond due to the slow speed of thermal diffusion. The solvent is thus thermally excited and the change in solvent structure is inversely related to the recombination dynamics of iodine.

These atomic motions were probed by X-ray diffraction for twenty time delays between 10 ps to 10 µs. The diffraction spectrum $S(q, \tau)$ depends on the momentum transfer $q = 4\pi \sin(\theta)/\lambda$ and the delay $\tau$. $2\theta$ is the scattering angle and $\lambda$ is the medium X-ray wavelength. The non-excited spectrum $S(q)$ for the $I_2/CCl_4$ solution and the laser induced signal is shown in Fig. 5. The feeble difference signal, shown in blue, is typically 1: 1000 of the total signal. Due to this weak signal everything in the experiments has to be stable: the X-ray and laser beam positions and intensities, the liquid jet and the detector. The intensity of the 3% pink beam on the sample was 5 x $10^8$ ph/s and the CCD detector was exposed for 10 s per image, limited by saturation of the liquid peak.
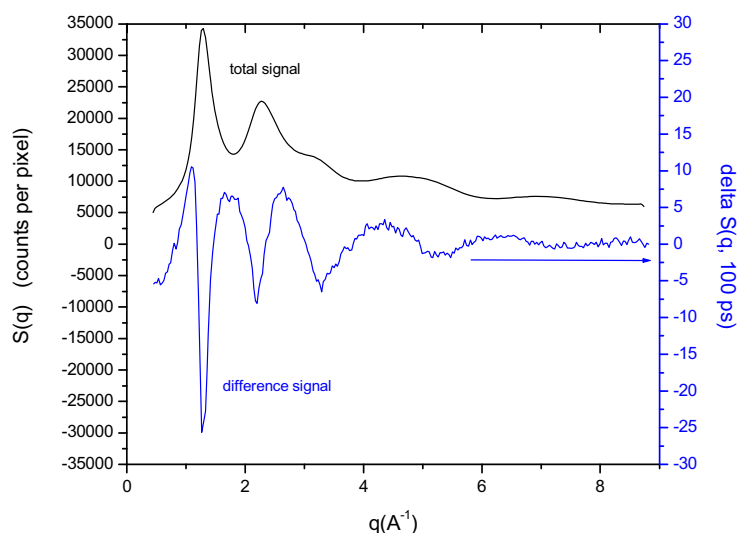
1191

**FIGURE 5.** The total signal from the $I_2/CCl_4$ solution is shown in the upper curve. The lower curve is the laser induced signal 100 ps after dissociation. In the q-range above 4 $A^{-1}$, S(q,100 ps) probes the changes in atom-atom correlations within molecules predominantly. At lower q < 4 $A^{-1}$, the oscillations stem predominantly from temperature changes in the solvent and changes in the packing of the solvent (cage effect). Note that the CCD records the full diffraction spectrum in one measurement.

The solution-phase diffraction spectrum probes all pairs of atoms in the solution. In fact the spectrum from a molecular liquid is naturally expressed by the atom-atom pair correlation functions $g_{\alpha\beta}$ (r, t) where $\alpha$ and $\beta$ are the types of atoms, i.e. I, C and Cl for $I_2/CCl_4$. If the atomic X-ray form factors is denoted by $f_\alpha(q)$, the scattering from the volume V is:

$$S(q,\tau) = \sum_{\alpha\beta} f_\alpha(q) f_\beta(q) \left( N_\alpha \delta_{\alpha\beta} + \frac{N_\alpha N_\beta}{V} \int_0^\infty g_{\alpha\beta}(r,\tau) \frac{\sin(q\,r)}{q\,r} 4\pi\,r^2\,dr \right) \tag{3}$$

$N_\alpha$ is the number of $\alpha$ atoms in the sample. In the absence of an analytical theory for molecular liquids, the $g_{\alpha\beta}$ functions are usually determined by Molecular Dynamics Simulations (MD), which are based on force-field models. Note that S(q, t) is the formfactor biased sum of the $g_{\alpha\beta}$ functions. In non-resonant X-ray scattering it is thus not possible to extract $g_{\alpha\beta}$ directly. The radial real-space Fourier transform is obtain by [8]:

$$\Delta S[r,\tau] \equiv \frac{1}{2\pi^2 r} \int_0^\infty dq \left[ \sum_{\mu\neq} \sum_\nu f_\mu(q) f_\nu(q) \right]^{-1} \times q\,\Delta S(q,\tau)\sin(qr) \tag{4}$$

which is the quantity used to interpret the data in real-space. It represents a formfactor-biased measure of the change in radial electron density seen by the average excited atom. When a series of snapshots are stitched together, it becomes a film of radial atomic motions during recombination. The $\Delta S[q, 100\ ps]$ and $\Delta S[r, 100\ ps]$ curves aer shown in Fig. 6. The first minimum in $\Delta S[r, 100\ ps]$ at 2.7 A comes from the depletion of the ground state X from the dissociation. The excited molecules then reach the A/A' and higher electronic states, and a maximum appears around 3.2A. In addition, the energy transfer from the solute to the solvent induces a rearrangement of the liquid without thermal expansion (isochoric temperature rise). The minima in $\Delta S[r, 100\ ps]$ at 4.0 and 6.2 A come from the changes in intermolecular Cl..Cl distances in $CCl_4$ that generated under isochoric conditions on the picosecond time scale. The transverse gradient in the laser beam leads to gradients in the temperature distribution in the liquid that lead to pressure gradients that eventually release through expansion. For a 100 µm laser beam, the speed of the pressure relaxation is proportional to the time it takes for sound to transverse the laser-illuminated volume, typically 50 ns. From the amplitude of the expansion, which typically leads to an increase in the nearest neighbor distances in

1192

the solvent of 1-5 mA and a 1-5 K temperature rise, the conservation of energy can be checked: is the observed temperature rise consistent with the chemical transitions used to explain the high-q data? In almost all reactions studied so far, the expansion is greater than the expected expansion from the observed structural transitions of the solutes. The discrepancy is usually attributed to fast and unresolved geminate recombination that injects energy into the solvent at times below 100 ps.
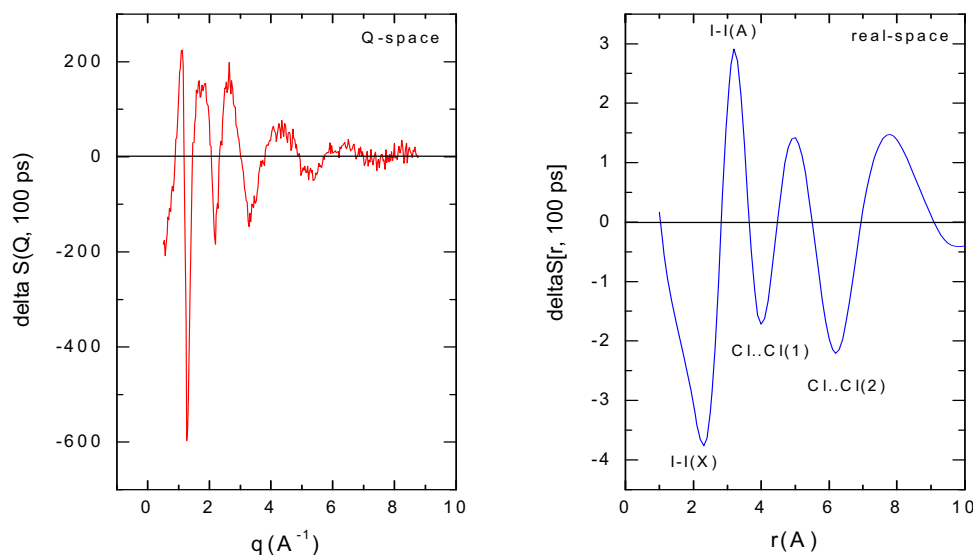


**FIGURE 6.** The laser induced signal from the dissociation of $I_2$ in $CCl_4$. The q-space is shown on the left and r-space on the right. The space curve is a measure of the change in the radial electron density for the average excited atom in the reaction.

Several chemical reactions have now been studied by solution phase X-ray diffraction. A new triangular C-I-C conformation of the $C_2H_4I$ radical was observed in the dissociation pathway for $C_2H_4I_2$ in methanol [11] and a novel linear isomer CH2I-I was observed in the dynamics of $CH_2I_2$ in methanol [12]. Common to these measurements is that diffraction always measures the sum of two components: the dynamics of the solutes in their cages and the heated solvent. It is impossible to separate the two contributions from one measurement. In some hydrogen containing solvents such a methanol and water, we have used the infrared beam from the femtosecond laser to excite overtones of hydrogen oscillations [13]. This technique does not produce any chemical change, only a transient temperature rise. The differential form of the solvent signal can be expressed as:

$$\Delta S(q,t) = \left(\frac{\partial S}{\partial T}\right)_\rho \Delta T(t) + \left(\frac{\partial S}{\partial \rho}\right)_T \Delta \rho(t), \tag{5}$$

a temperature derivative at constant density (or volume) and a density differential at constant temperature. Note that the coefficients are time dependent and determined by the energetics of the chemical reaction (not the structural change of the solutes) and the hydrodynamic parameters of the solvent. Armed with these differentials, the structures of the caged solutes is usually readily determined as discussed in reference [13].

## OUTLOOK

The 100 picosecond time resolution of third generation synchrotrons makes is impossible to visualize the primary steps in bond breakage and bond formation. These processes take place on the time scale of molecular vibrations, i.e. in 0.1-1 ps. These times and below will become accessible with the X-ray Free Electron Lasers (XFEL) that are under construction or in an advanced stage of design. Flux comparisons with synchrotron sources indicate that

1193

single-shot experiments with $1 \times 10^{12}$ ph per pulse at 12.4 keV will become possible with unprecedented signal to noise. The actual laser/X-ray time delay will need to be measured for every single shot to compensate for the expected synchronization jitter of 1 ps (rms). However sorting the data after the experiment in time bins followed by averaging should allow to resolve ultrafast phenomena to 100 fs resolution and perhaps below. Note that the propagation velocity of optical light is slower than for X-rays. That implies that future XFEL samples will have to be thin, typically 20 um, to maintain a well-defined time delay during the passage of the two co-linear pulses.

There is an obvious advantage in having ultrafast time resolution. It will become possible to see the *order of events* in chemical and biochemical reactions. In the photo dissociation process of CO in Myoglobin, which might be studied using Laue diffraction from a spontaneous undulator at an XFEL facility, we will see how long it takes for the CO molecule to reach the first docking site. And once there, how and when do neighboring residues respond to the new space constraints?

At synchrotrons the total flux of a given undulator harmonic is essentially proportional to the bunch charge, the number of periods of the undulator and the pulse frequency. At the ESRF it is not possible to increase the bunch charge beyond 15-30 nC since that is detrimental to the emittance and lifetime. There is a potential gain of 3 in using all three sides of the ESRF chopper and such a chopper is being commissioned. Simulations show that if the center of mass and the geometrical center coincide to 10 μm, the thee sides of the rotor can be used to chop the beam at 3 kHz in for time modes with bunch spacing greater than ~ 176 ns (16 bunch mode). A 3 kHz chopper would increase the flux by 3 and hence shorten the exposure time likewise. More importantly, the 3 kHz option will allow us to work at energies where the flux is lower. Finally a heat load chopper is being installed in the optics hutch upstream the monochromator and the mirror. It consists of a 200 mm diameter Cu wheel with five 4 mm high tunnels through the center. When it rotates at 100 Hz, it produces 80 μs pulses at 1 kHz. It promises to lower the heatload on the optics and the chopper by a factor 12.5. The resulting improved stability of the focused beam should make it possible to use longer exposures with improved signal to noise, which will hopefully resolve new fine structure of molecules in action.

## ACKNOWLEDGMENTS

## REFERENCES

1. Y.R. Shen, "The Princiles of Nonlinear Optics": Wiley, New York, 1984.
2. M. H. Pirenne, "The Diffraction of X-rays and Electrons by Free Molecules", Cambridge University Press, 1946,
3. H. Ihee et al., "Direct imaging of transient molecular structures with ultrafast diffraction", Science, 291, 458-462 (2001).
4. J.R. Helliwell and P.M. Rentzepis. "Time-resolved Diffraction". Oxford Series on Synchrotron Radiation, No. 2. Oxford University Press, Oxford, 1997.
5. C. Bressler and M. Chergui. "Ultrafast X-ray absorption spectroscopy". Chem. Rev., 104(4): 1781-1812 (2004).
6. A.M. Lindenberg *et al. Science*, 308, 392 (2005).
7. L. Eybert, M. Wulff, W. Reichenbach, A. Plech, F. Schotte, E. Gagliardini, L. Zhang, O. Hignette, A. Rommeveaux and A. Freund. "The toroidal mirror for single-pulse experiments on ID09B". SPIE Vol. 4782, p 246-257 (2002).
8. Plech, M. Wulff, S. Bratos, F. Mirloup, R Vuilleumier, F. Schotte and P.A. Anfinrud. "Visualising Chemical Reactions in Solution by Picosecond X-ray Diffraction", Physical Review Letters, vol 92, no 12, 125505-1 to 125505-4 (2004).
9. S. Rice, Nature, Vol 429, p 255 (2004).
10. M. Wulff, S. Bratos, A. Plech, R. Vuilleumier, F. Mirloup, M. Lorenc, Q. Kong, H. Ihee. "Recombination of Photo-dissociated Iodine: A time-resolved X-ray Study" Journal of Chemical Physics, 124, 34501-34513 (2006).
11. H. Ihee, M. Lorenc, T. K. Kim, Q. Y. Kong, M. Cammarata, J. H. Lee, S. Bratos, M. Wulff, "Ultrafast X-ray Diffraction of Transient Structures in Solution", Science, 309, 1223-1227 (2005).
12. J. Davidsson, J. Poulsen, M. Cammarata, P. Georgiou, R. Wouts, G. Katona, F. Jacobson, A. Plech, M. Wulff, G. Nyman and R. Neutze, "Structural Determination of a Transient Isomer of $CH_2I_2$ by Picosecond X-Ray Diffraction", Physical Review Letters 94, 245503 (2005).
13. M. Cammarata, M. Lorenc, T. K. Kim, J. H. Lee, Q. Y. Kong, E. Pontecorvo, M. Lo Russo, G. Schiró, A. Cupane, M. Wulff, H. Ihee. "Impulsive solvent heating probed by picosecond x-ray diffraction". Journal of Chemical Physics, 124, 124504, 2006.